

# RNA-sequencing in ophthalmology research: considerations for experimental design and analysis

Nicholas Owen and Mariya Moosajee 

**Abstract:** High-throughput, massively parallel sequence analysis has revolutionized the way that researchers design and execute scientific investigations. Vast amounts of sequence data can be generated in short periods of time. Regarding ophthalmology and vision research, extensive interrogation of patient samples for underlying causative DNA mutations has resulted in the discovery of many new genes relevant to eye disease. However, such analysis remains functionally limited. RNA-sequencing accurately snapshots thousands of genes, capturing many subtypes of RNA molecules, and has become the gold standard for transcriptome gene expression quantification. RNA-sequencing has the potential to advance our understanding of eye development and disease; it can reveal new candidates to improve our molecular diagnosis rates and highlight therapeutic targets for intervention. But with a wide range of applications, the design of such experiments can be problematic, no single optimal pipeline exists, and therefore, several considerations must be undertaken for optimal study design. We review the key steps involved in RNA-sequencing experimental design and the downstream bioinformatic pipelines used for differential gene expression. We provide guidance on the application of RNA-sequencing to ophthalmology and sources of open-access eye-related data sets.

**Keywords:** bioinformatics, differential gene expression, false discovery rate, gene ontology, next-generation sequencing, ophthalmology, power, replicates, RNA-sequencing, transcriptomics

Received: 3 October 2018; accepted in revised form: 8 February 2019.

## Introduction

With the advent of high-throughput sequencing technologies, focus on temporal gene expression through examination of the active transcriptome of tissues, cells, and model systems using RNA-sequencing (RNA-seq) has increased.<sup>1</sup> In ophthalmology and vision research, RNA-seq utilization is extensive. For example, investigation of gene expression changes in corneal epithelial tissue from keratoconus patients has provided insights into the cause of this progressive corneal degeneration.<sup>2</sup> Pathways including Wnt, Hedgehog, and Notch1 signaling were shown to be significantly reduced in keratoconus epithelium. In glaucoma, the leading cause of irreversible blindness worldwide characterized by the progressive loss of retinal ganglion cells (RGCs),<sup>3,4</sup> investigations into the RGC transcriptome of induced pluripotent stem cells (iPSCs) from patients with the *SIX6* risk allele [missense

variant rs33912345; C>A; p.(His141Asn)] associated with reduced retinal nerve fiber layer thickness, and mouse models of optic nerve head damage have identified critical pathophysiologic pathways, such as endoplasmic reticulum stress, Notch signaling, and mammalian target of rapamycin (mTOR) pathway.<sup>5–7</sup> Elucidation of transcript signatures in lens development has revealed the expression of novel transcripts decreasing in post-natal tissue.<sup>8</sup> Lens-enriched expression analysis has confirmed high expression of established cataract-linked genes, such as the *Crystallin* gene family, and identified a number of transcription factors as novel potential regulators in the lens.<sup>9</sup> RNA-seq of rod photoreceptors from the zebrafish has identified novel expression of genes not previously thought to be expressed in this cell type including *opsin 4.1* and several nuclear hormone receptor genes.<sup>10</sup> Similar experiments on dissociated mouse cones

*Ther Adv Ophthalmol*

1–23

DOI: 10.1177/  
2515841419835460

© The Author(s), 2019.  
Article reuse guidelines:  
sagepub.com/journals-  
permissions

Correspondence to:

**Mariya Moosajee**  
Development, Ageing  
and Disease Theme, UCL  
Institute of Ophthalmology,  
University College London,  
11–43 Bath Street, London  
EC1V 9EL, UK.

[m.moosajee@ucl.ac.uk](mailto:m.moosajee@ucl.ac.uk)

**Nicholas Owen**  
Development, Ageing  
and Disease Theme, UCL  
Institute of Ophthalmology,  
University College London,  
London, UK

**Mariya Moosajee**  
Development, Ageing  
and Disease Theme, UCL  
Institute of Ophthalmology,  
University College London,  
London, UK  
NIHR Biomedical Research  
Centre for Ophthalmology,  
Moorfields Eye Hospital  
NHS Foundation Trust,  
London, UK  
Great Ormond Street  
Hospital for Children NHS  
Foundation Trust, London,  
UK

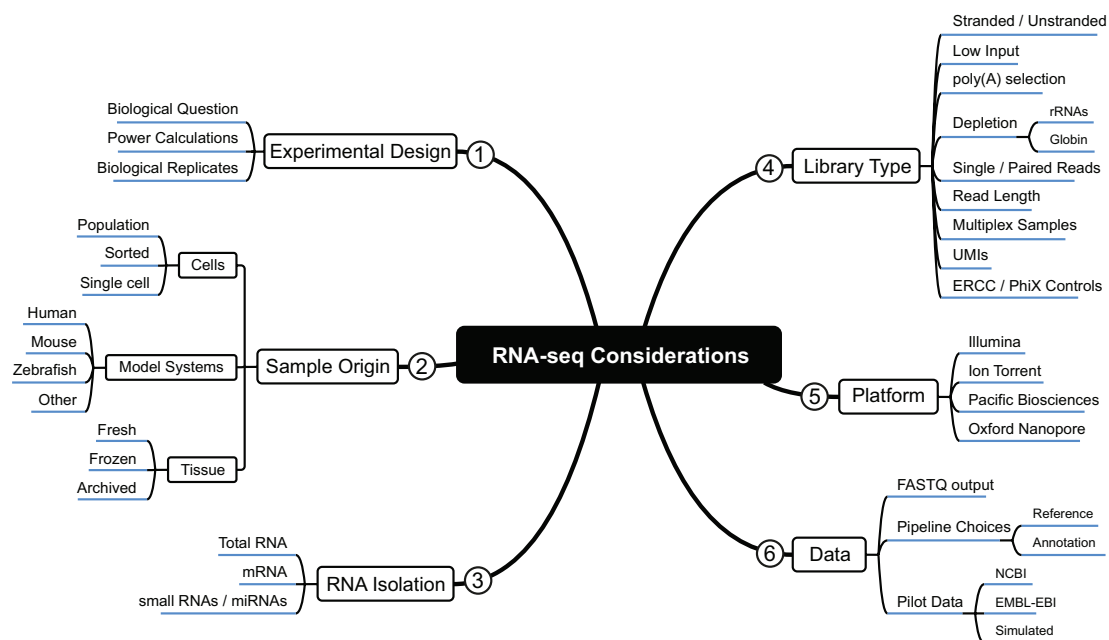


**Figure 1.** A diagrammatic overview of the considerations for designing a successful RNA-seq experiment for differential gene expression analysis. Branches of the outline are numbered to indicate the general order for the considerations. Within each branch, subbranches denote options to consider within the design.

have provided an insight into the gene expression patterns occurring throughout postnatal development, highlighting 14% of all genes detected were switched off around postnatal day 6 (P6), including those encoding transcription factors, neurogenesis, and cone-specific genes.<sup>11</sup> Such investigations reveal the role of previously unknown or unclassified transcripts in eye development, for example, the characterization of zebrafish *zic2*, which restricts *pax2a* expression and Hedgehog signaling, when ablated causes chorioretinal coloboma<sup>12</sup> and identification of numerous miRNAs regulating pathways not previously associated with retinal degeneration, using retinal pigment epithelium (RPE) cells under oxidative stress as a model system.<sup>13</sup> In this manner, novel information is gleaned; new targets for potential molecular diagnosis or therapeutic interventions may emerge.<sup>14,15</sup> In this review, we will cover the considerations for the design and execution of a typical RNA-seq project investigating differentially expressed messenger RNA (mRNA). We will provide recent examples of the utilization of RNA-seq within the field of ophthalmology.

### Considerations for RNA-seq experimental design

With no single optimal pipeline for this experimentation, combined with no standard application and analysis approach, the use of RNA-seq

data can be daunting. Experimental plan and strategic approaches depend highly on the type of RNA and or organism being studied, as well as the goals of the research. One may utilize previously reported species transcriptomes to guide the alignment of reads or align without prior knowledge to identify potentially novel transcripts.

One of the most crucial requirements for a successful RNA-seq experiment is the biological question of interest and how the data generated can answer that. Figure 1 summarizes critical aspects for an optimal experimental design. Number of sample replicates is of importance as increasing the number per biological condition has a more significant impact on the accuracy of the data produced over increasing sequencing depth.<sup>16,17</sup> A growing number of algorithms can calculate the required sample number for significance and power of experiments; including Scotty,<sup>18</sup> powsimR,<sup>19</sup> PROPER,<sup>20</sup> and RNASeqPower.<sup>21</sup> Technical replicates are generally not required for differential expression analysis, as RNA-seq has been shown to be accurate as well as reproducible.<sup>22–24</sup>

For pilot studies to assess accuracy and variance of analysis at different stages of an RNA-seq pipeline, simulated data can be created through synthetic reads generated from genomic sequence.<sup>25,26</sup> It is also possible to utilize transcriptomic data

**Table 1.** Summary of a subset of NCBI-submitted RNA-seq experimental data sets related to eye development and disease, highlighting utilized methods and software. The NCBI Gene Expression Omnibus (GEO) was searched for terms 'retina disease; retina development; eye disease; eye development', subsetting on 'Study type' - 'expression profiling by high throughput sequencing' (December 2018) (available details of the software used for analysis are noted; \* unpublished data sets).

Keywords	Data set description	Species	NCBI GEO	Software	Reference
Cornea	Molecular Effects of Doxycycline Treatment on Pterygium as Revealed by Massive Transcriptome Sequencing	<i>Homo sapiens</i>	GSE34736	Tuxedo: TopHat2, Cufflinks2	Larrayoz and colleagues <sup>29</sup>
Cornea	RNA-seq analysis in Cornea epithelial cells (CECs), skin epithelial cells (SECs), LSCs after knocking down PAX6 (3-D shPAX6 LSCs) and SESCOs transduced with PAX6 (3-D PAX6+SECOs) upon 3-D differentiation	<i>H. sapiens</i>	GSE54322	Not reported	Ouyang and colleagues <sup>30</sup>
Cornea	Molecular Effects of Doxycycline Treatment on Pterygium from Caucasian Patients as Revealed by Massive Transcriptome Sequencing	<i>H. sapiens</i>	GSE58441	Tuxedo: TopHat2, Cufflinks2	Larrayoz and colleagues <sup>29</sup>
Cornea	RNA-seq analysis and comparison of corneal epithelium in keratoconus and myopia patients	<i>H. sapiens</i>	GSE112155	TopHat2, edgeR, DESeq2, limma	You and colleagues <sup>2</sup>
Cornea	RNA Mis-splicing in Fuchs Endothelial Corneal Dystrophy II	<i>H. sapiens</i>	GSE112201	TopHat2, edgeR	Wieben and colleagues <sup>31</sup>
Cornea	RNA Mis-splicing in Fuchs Endothelial Corneal Dystrophy	<i>H. sapiens</i>	GSE101872	TopHat2, edgeR	*
Cornea	Transcriptome profiling of human keratoconus corneas through RNA-sequencing identifies collagen synthesis disruption and downregulation of core elements of TGF- $\beta$ , Hippo, and Wnt pathways	<i>H. sapiens</i>	GSE77938	Bowtie2, String Tie, Cufflinks2, Kallisto, DESeq2, edgeR	Kabza and colleagues <sup>32</sup>
Diabetic retinopathy	Transcriptomic Analysis of Endothelial Cells from Fibrovascular Membranes in Proliferative Diabetic Retinopathy	<i>H. sapiens</i>	GSE94019	Partek	*
Muller glia	Rapid, dynamic activation of Müller glial stem cell responses in zebrafish	<i>Danio rerio</i>	GSE86872	RSEM, edgeR, limma	Sifuentes and colleagues <sup>33</sup>
Retina	Id2a knockdown in zebrafish retina	<i>D. rerio</i>	GSE38786	Bowtie, DESeq, DAVID	Uribe and colleagues <sup>34</sup>
Retina	Molecular anatomy of the developing human retina	<i>H. sapiens</i>	GSE104827	STAR, RSEM, limma,	Hoshino and colleagues <sup>35</sup>
Retina	The Dynamic Epigenetic Landscape of the Retina During Development, Reprogramming, and Tumorigenesis	<i>H. sapiens</i>	GSE87042	TopHat2, Cufflinks2	Aldiri and colleagues <sup>36</sup>

(Continued)

Table 1. (Continued)

Keywords	Data set description	Species	NCBI GEO	Software	Reference
Retina	Unprecedented alternative splicing and 3 Mb of novel transcribed sequence leads to significant transcript diversity in the transcriptome of the human retina	<i>H. sapiens</i>	GSE40524	RUM pipeline	Farkas and colleagues <sup>15</sup>
Retina	Comparative Systems Pharmacology of HIF Stabilization in the Prevention of Retinopathy of Prematurity	<i>Mus musculus</i>	GSE74170	TopHat, Cufflinks	Hoppe and colleagues <sup>37</sup>
Retina/CRX	Graded Expression Changes Determine Phenotype Severity In Mouse Models of CRX-Associated Retinopathy	<i>M. musculus</i>	GSE45506	TopHat, edgeR	Ruzycski and colleagues <sup>38</sup>
Retina/Macula	Comprehensive analysis of gene expression in human retina and supporting tissues	<i>H. sapiens</i>	GSE94437	GSNAP, Cufflinks2	*
Retina/RP	rd10 transcriptome analysis	<i>M. musculus</i>	GSE56473	RMap, edgeR	Uren and colleagues <sup>39</sup>
Retina/RPE	Comprehensive analysis of gene expression in human retina and supporting tissues	<i>H. sapiens</i>	GSE94437	GSNAP, Cufflinks2	*
Retina/RPE	Region-specific Transcriptome Analysis of the Human Retina and RPE/Choroid	<i>H. sapiens</i>	PRJNA336370	TopHat2, Cufflink2, cummeRbund	Whitmore and colleagues <sup>40</sup>
Retina/RPE/ES	Comparative transcriptomic analysis of self-organized, in vitro generated optic tissues	<i>M. musculus</i>	GSE62432	TopHat2, Cufflinks2, edgeR	Andrabi and colleagues <sup>41</sup>
Retinoblastoma	A three-dimensional organoid model recapitulates tumorigenic aspects and drug responses of advanced human retinoblastoma	<i>H. sapiens</i>	GSE120710	Kallisto	Saengwimol and colleagues <sup>42</sup>
Retinal Culture/iPSC	Treatment Paradigms for Retinal and Macular Diseases Using 3-D Retina Cultures Derived From Human Reporter Pluripotent Stem Cell Lines	<i>H. sapiens</i>	GSE103826	Not reported	Kaewkhaw and colleagues <sup>43</sup>
Retinal Culture/iPSC	Transcriptome dynamics of developing photoreceptors in 3-D retina cultures recapitulates temporal sequence of human cone and rod differentiation revealing cell surface markers and gene networks	<i>H. sapiens</i>	GSE67645	Bowtie2, eXpress, edgeR, limma	Kaewkhaw and colleagues <sup>44</sup>
Retinal Culture/iPSC/ESC	Accelerated and Improved Differentiation of Retinal Organoids from Mouse Pluripotent Stem Cells in Rotating-Wall Bioreactors	<i>M. musculus</i>	GSE102727	edgeR, limma	DiStefano and colleagues <sup>45</sup>
RGC/ESC	Enriched retinal ganglion cells derived from human embryonic stem cells (RNA-seq)	<i>H. sapiens</i>	GSE84639	ExAtlas	Gill and colleagues <sup>46</sup>
RPE	Aneuploidy-induced cellular stresses limit autophagic degradation.	<i>H. sapiens</i>	GSE40570	RSEM, Bowtie, DESeq, ssGSEA	Santaguida and colleagues <sup>47</sup>

Table 1. (Continued)

Keywords	Data set description	Species	NCBI GEO	Software	Reference
RPE	Regulation of protein translation during mitosis	<i>H. sapiens</i>	GSE67902	Bowtie, DAVID	Tanenbaum and colleagues <sup>48</sup>
RPE	RNA-Seq analysis of 4N and 2N RPE1 cells following polyploid induction via cytokinesis failure or Aurora kinase inhibition [tpo3]	<i>H. sapiens</i>	GSE86101	TopHat2, edgeR	Potapova and colleagues <sup>49</sup>
RPE	RNA-Seq analysis of proliferating 4N and 2N RPE1 cells derived from single cell clones following inhibition of Aurora B to induce polyploidization [tpo10]	<i>H. sapiens</i>	GSE86103	TopHat2, edgeR	Potapova and colleagues <sup>49</sup>
RPE	RNA-Seq analysis RPE1 cells following exposure to Nutlin-3 to identify target genes of p53 [tpo12]	<i>H. sapiens</i>	GSE86104	TopHat2, edgeR	Potapova and colleagues <sup>49</sup>
RPE	Appropriately Differentiated ARPE-19 Cells Regain a Native Phenotype and Similar Gene Expression Profile	<i>H. sapiens</i>	GSE88848	CLC Genomics Workbench, DESeq2	Samuel and colleagues <sup>50</sup>
RPE/AMD	Reversal of persistent wound-induced retinal pigmented epithelial-to-mesenchymal transition by the TGF $\beta$ pathway inhibitor, A-83-01	<i>H. sapiens</i>	GSE67898	Partek, edgeR	Radeke and colleagues <sup>51</sup>
RPE/AMD	A widespread decrease of chromatin accessibility in age-related macular degeneration	<i>H. sapiens</i>	GSE99287	TopHat2, Cufflinks2	Wang and colleagues <sup>52</sup>
RPE/iPSC	Expression data for hiPSC-derived RPE treated with 10mM Nicotinamide or vehicle	<i>H. sapiens</i>	GSE90889	STAR, bedtools, samtools, DESeq2	Saini and colleagues <sup>53</sup>
RPE/iPSC	Comparison of stem-cell derived retinal pigment epithelia (RPE) with human fetal retina pigment epithelium	<i>H. sapiens</i>	GSE36695	Galaxy - TopHat2, Cufflinks2	*

AMD, age-related macular degeneration; DAVID, Database for Annotation, Visualization, and Integrated Discovery; iPSC, induced pluripotent stem cell; NCBI, National Center for Biotechnology Information; RGS, retinal ganglion cell; RNA-seq, RNA-sequencing; RP, retinal pigment; RPE, retinal pigment epithelia.

submitted to public repositories, such as EMBL ENA<sup>27</sup> and National Center for Biotechnology Information (NCBI) SRA,<sup>28</sup> to obtain information on the variance of data. Table 1 summarizes the current obtainable experimental RNA-seq data sets related to ophthalmology and vision research at NCBI. Combination of data with published data sets from different biological samples, sequencing centers, or varying experimental protocols may lead to incorporation of batch effects. Such meta-analysis, therefore, would have decreased statistical power and accuracy, even in well-designed studies.<sup>54</sup> A significant source of false discovery of differential expression is commonly across batches of experiments rather than across the biological groups of interest.<sup>55</sup>

#### *RNA isolation*

Within our cells, several RNA species are present at any one time serving differing roles. Through transcription of genes, there are protein-encoding mRNAs. Small RNAs involved in translation include transfer RNAs (tRNAs) and ribosomal RNAs (rRNAs). Regulatory RNA species, include antisense RNAs (asRNAs), microRNAs (miRNAs), Piwi-interacting RNAs (piRNAs), small interfering RNAs (siRNAs), short hairpin RNA (shRNA), and long noncoding RNA (lncRNA), all play a role in gene expression regulation. Highly abundant rRNA species, the predominant component of the ribosome involved in protein synthesis, constitutes up to 90% of the total RNA in cells. rRNA may require removal from samples to produce a library with considerably more representation of mRNA transcripts. Methods for rRNA removal include enriching mRNA using poly(A) selection, targeting the polyadenosine monophosphates at the 3' tail of mature mRNA species, or depletion of rRNA by systems such as Ribo-Zero (Illumina, CA, USA) and duplex-specific nuclease degradation.<sup>56</sup> rRNA depletion is an essential consideration for formalin-fixed and paraffin-embedded (FFPE) samples where RNAs are potentially degraded to a small average size, under 200 nucleotides.<sup>57</sup> rRNA depletion should also be considered when the biological sample cannot provide enough quantity or high-quality mRNA through poly(A) selection.<sup>58,59</sup> For samples with a small amount of starting material, there are specific library preparation systems available, such as SMART-seq (Takara Bio, CA, USA), relying on pre-amplification of fragments and may include a second stage of amplification.<sup>60</sup> This can result in variable 3' end bias

representation of genes in library preparation, although the overall effect on expression values may be negligible.<sup>61</sup> Small RNA species, such as those lacking poly(A) signals, can be assessed through small RNA-seq protocols.<sup>62</sup>

#### *Library preparation and platforms*

To convert RNA into a library of molecules for sequencing, generally, it is first fragmented to an appropriate size for the chosen platform, either by physical or enzymatic approaches. First-strand complementary DNA (cDNA) is synthesized from the RNA sequences. Dependent on the platform and library kit used, platform-specific adapter sequences may be incorporated to the ends of the molecules to enable subsequent sequencing. Some systems add adapter sequences through ligation after cDNA synthesis (including Illumina TruSeq, Takara Clontech SMARTer, PerkinElmer NEXTFlex, and KAPA Biosystems); other sequences may be attached to each molecule, including an inline index to identify the sample, allowing multiplexing of libraries when sequencing. Inline barcodes can be utilized to provide a label of origin for each RNA molecule.<sup>63</sup> Recent developments include unique molecular identifiers (UMIs), molecular tags consisting of several random bases that can be used to detect and quantify unique transcripts.<sup>63–65</sup> Unwanted duplication of reads through amplification methods can readily be detected.<sup>66,67</sup> The addition of UMIs significantly improves the accuracy of gene quantification, especially high expressing genes.<sup>68,69</sup> The resulting library of cDNA molecules can then be assessed for quality before sequencing.

For library preparation, one must consider how much RNA will be available for the experiment as well as the specific library types required, for example, those that maintain strand information or need significantly lower input RNA levels, such as those from FFPE or laser-captured micro-dissected samples,<sup>70</sup> and single-cell RNA-seq (scRNA-seq).<sup>71</sup> Strand-specific RNA-seq can resolve the ambiguity of overlapping genes transcribed on opposite strands, allowing identification of antisense expression by retaining information from which DNA strand the RNA was first transcribed.<sup>72</sup> This information can be maintained using approaches that either incorporate a chemical modification in the second cDNA synthesis stage, with subsequent digestion of the nonmodified strand, or incorporate distinct

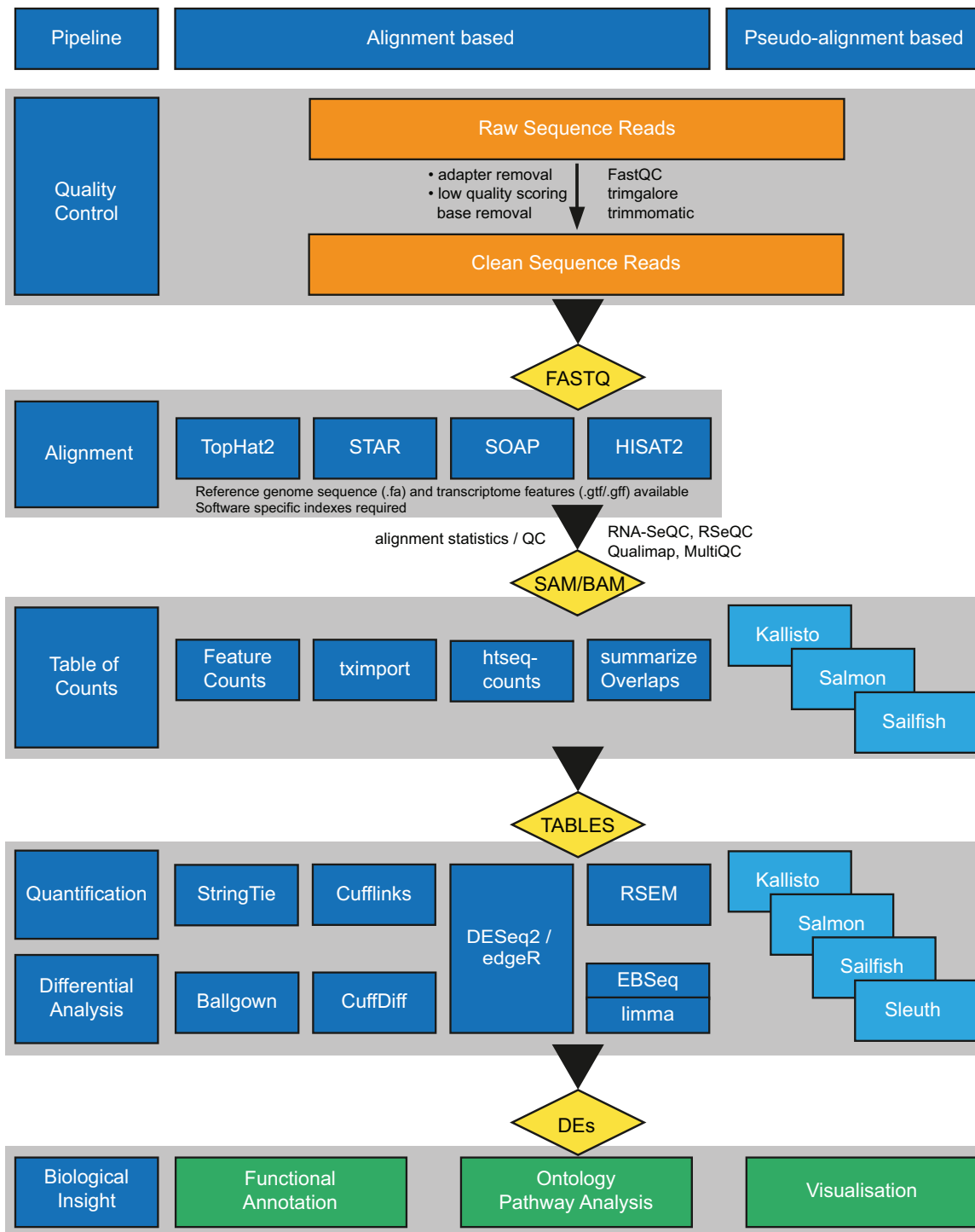


**Figure 2.** Schematic representation of typical bioinformatic processing of high-throughput sequence data for RNA-seq experiments. The sequencing platform generated raw reads (FASTQ) are subjected to quality assessment. Where a reference genome and a high-quality annotation are available, resulting high-quality cleaned reads can be used in alignment- or pseudo-alignment-based processes. For alignment-based process, reads are mapped to the genome and transcriptome in a splice-aware manner. Resulting alignments (SAM/BAM/CRAM) are assessed for mapping qualities and counts of features (genes/transcripts/exons) generated. Counts are modeled for quantification and differential analysis computed using various methods, resulting in differential feature lists. With pseudo-alignment-based methods, clean reads are modeled to the transcriptome, allowing direct quantification of appropriate feature(s) for differential analysis. The output of

**Figure 2.** (Continued)

both approaches can provide further insight through gene ontology analysis (GSEA/GO ORA), pathway analysis (Panther, KEGG, DAVID), and visualized (IGV, GenomeBrowse, Bioconductor) for report production. Software examples listed are non-exhaustive.

DAVID, Database for Annotation, Visualization, and Integrated Discovery; GO, gene ontology; GSEA, gene set enrichment analysis; IGV, Integrative Genomics Viewer; KEGG, Kyoto Encyclopedia of Genes and Genomes; ORA, over-representation analysis; Panther, Protein Analysis Through Evolutionary Relationships; SAM/BAM, sequence/binary alignment map.

primer adapters with the RNA.<sup>73,74</sup> Library preparation protocols differ to achieve specific goals; TruSeq™ (Illumina) is a general method chosen when starting material is not restricted; Smart-Seq2 and Ovation (NuGen, CA, USA) are suited to low input amounts.<sup>60,70,75</sup>

High-throughput sequencing approaches are rapidly evolving regarding both technology and chemistry. Illumina, PacBio RS, Oxford Nanopore, and Ion Torrent are some of the most commonly utilized platforms.<sup>76,77</sup> The Illumina short read ‘sequence-by-synthesis’ systems have been rapidly adopted by the research community due to high data throughput, accuracy, availability, and declining costs.

**Sequencing**

Sequencing depth, the number of fragments sequenced per sample, remains a critical factor for RNA-seq design. Studies have reported that increasing reads does not always provide increased biological significance.<sup>16,17</sup> However, detection of lower abundance RNA species requires increased read sequencing, although RNA-seq shows a greater dynamic range than other assays.<sup>78,79</sup> For the analysis of differential gene expression alone in human samples, 10–20 million reads per sample would provide significant information on most genes expressed. Investigation of alternatively spliced, novel isoforms, or fusion events, will require higher read number to capture the expression patterns, although increasing reads are associated with increased noise.<sup>17</sup>

With the depth of sequencing and library construction, comes the considerations of single-end reads or paired-end reads and read length. cDNA products may be sequenced from either single or both ends (paired). For simple differential expression analysis, single-end reads can provide valuable information. Paired-end reads, due to the size of RNA fragments produced (typically 300–500 nucleotides), will provide more

significant information as the number of reads from fragments spanning exon–intron boundaries will be higher. As RNA-seq investigates transcribed and processed RNA, it is crucial that a level of aligned reads or paired-end fragments span exon boundaries. Single-end reads can be utilized for analysis of the 3′ regions of transcripts, such as with Tag-seq and MACE, assuming expression as a whole from sequencing the end region only.<sup>80</sup>

There are several biases in the analysis of RNA-seq differential expression: low-level transcripts producing high significance in expression-level differences and longer more abundant transcripts showing greater significance due to large number of reads per library aligned to their reference sequence. Read length is highly dependent on the application; for gene expression, profiling short reads (50–75 basepairs, bp) will detect the majority of RNA species in a library; for analysis of the transcriptome including identification of novel annotations, paired-end reads of 100+ bp will enable complete coverage of transcripts and novel splice sites; and for small RNA analysis, a read length of 50 bp would provide coverage of the majority of RNA due to their size. Long read sequencing is also possible using systems including PacBio and Oxford Nanopore, providing detailed analysis of specific isoforms expressed as well as allele-specific expression patterns, allowing the development of personalized transcriptomes.<sup>81</sup>

**RNA-seq analysis at the mRNA level**

Commonly, RNA-seq experiments investigating differential gene expression follow the stages outlined in Figure 2. Once sequencing data are generated, it requires alignment to either the genome or transcriptome reference sequences. In situations where novel transcripts are of interest, alignment to the genome followed by *de novo* transcript assembly is required. After alignment, feature counts are calculated and normalized, and



differentially expressed features are identified. How these changes are biologically relevant to the experimental hypothesis is the final stage of investigation.

There are an increasing number of tools and methods of analysis for RNA-seq data sets, with each stage of the study requiring appropriate quality control. Aside from command-line tools and cloud-based approaches, commercial products include CLC Genomics Workbench (Qiagen, CA, USA), DNAnexus, Ingenuity IPA (Qiagen), and Partek Genomics Suite. Software for differential expression analysis has been evaluated using both experimental and simulated data sets. Comprehensive reports of such tools have been presented previously.<sup>82–85</sup> Combination of approaches using different tools has led to improved results.<sup>86</sup> Therefore, it is recommended to utilize multiple pipelines on the data set and understand fully the differences and similarities in the results. For this review, we will focus on several commonly cited, free, open-source tools to achieve differential expression analysis of human samples. The tools mentioned are not intended as an extensive list.

#### Read quality control

The Illumina sequencing platform will produce raw FASTQ files that represent the sequence of the library in question. FASTQ is a text-based file format including all the sequence data along with associated quality scores. Each Phred score represents a log-scaled estimated probability of error in the base being called, for example, a score of 30 indicates a 1 in 1000 probability that the base is incorrect. Initial processing of these read files should include quality assessment of the base calls using tools such as FASTQC<sup>87</sup> or FASTX-Toolkit.<sup>88</sup> These provide graphical summaries of the sample reads, allowing quick visual identification of potential problems. Issues may commonly include over-represented sequences (e.g. adapter sequences or rRNA) or low-quality scoring bases at the 3' end of reads. Tools to process the reads, filtering of poor bases, and trimming bases and adapters include Trimmomatic,<sup>89</sup> Trim Galore,<sup>90</sup> and cutadapt.<sup>91</sup>

#### Read alignment

Post-processing of the cleaned FASTQ reads requires either alignment to the human genome, such as Ensembl GRCh38 or NCBI hg38 builds,

or the associated human transcriptome or pseudo-alignment to the transcriptome and count modeling with tools such as Salmon,<sup>92</sup> Kallisto,<sup>93</sup> and Sailfish.<sup>94</sup> Alignment of reads requires software that can process mapping in a splice-aware manner.<sup>95,96</sup> Many reads generated will span splice junction coordinates, and alignment will require algorithms to split reads to different exonic positions. Mapping software includes HISAT2,<sup>97</sup> SOAPsplice,<sup>98</sup> TopHat2,<sup>99</sup> and STAR.<sup>100</sup> These produce a sequence/binary alignment map (SAM/BAM<sup>101</sup>) file of the reads aligned to the genome. Alignments may be visualized using tools such as Integrative Genomics Viewer (IGV)<sup>102,103</sup> or GenomeBrowse,<sup>104</sup> providing an insight to read metrics at the feature level. One of the greatest challenges is the subsequent assignment of aligned reads to transcripts they originate from to infer gene expression. Several new generation tools have introduced alignment-free transcript or gene quantification methods.<sup>92–94</sup> These utilize *k*-mer-based matching to indexed transcript data sets, breaking reads into smaller *k*-mers, resulting in significantly faster analysis.<sup>94</sup> A recent report, while confirming different pipeline performance was virtually identical for *in vivo* transcripts, demonstrated that alignment-based approaches were superior to alignment-free pipelines for total RNA analysis, as both small genes and low-expressed genes biased the accuracies of alignment-free approaches.<sup>105</sup>

#### Read duplication

Post alignment, processing of the data includes sorting by genomic coordinates and marking reads that can be assigned as optical or polymerase chain reaction (PCR) duplicates,<sup>106,107</sup> using tools such as Picard.<sup>108</sup> There is significant discussion as to whether such reads should be removed from the analysis, as preferential amplification of cDNA fragments in the library preparation could result in a gene/isoform having an increased level of reported expression if such duplicated fragments were included.<sup>109,110</sup> Other biases can consist of fragment GC-content, priming of reverse transcription by random hexamers, and rRNA depletion methods.<sup>70,111,112</sup> A common practice to handle PCR duplicates would include removal of all but one representative read of identical sequences; however, this assumes that all identical reads were generated by PCR from the sample cDNA molecule.<sup>113</sup> If removed, biologically significant information

may be lost as smaller genes have reads that span the same genomic coordinates. UMIs enable tracking of fragments through library preparation, sequencing, and data analysis to overcome such biases.<sup>66,114</sup>

#### *Feature summarization*

Expression levels of features, either at the gene or transcript level, are estimated from mapped read counts where appropriate feature annotation files exist. There is currently no consensus approach that is the most suitable to all situations, although this is an area of significant recent development.<sup>85</sup> Initial analysis of RNA distribution through technical replicates fitted well to a Poisson distribution, in which reads map to the transcriptome in a random unrelated fashion within the library.<sup>22,115,116</sup> With decreasing cost and speed, the use of higher numbers of biological replicates demonstrated that sample variability was greater than the expected distribution, giving increased false positives. Subsequent methods to handle this variability include analysis based on negative and beta-negative binomial statistical models, such as edgeR,<sup>117</sup> BaySeq,<sup>118</sup> Cufflinks2,<sup>119,120</sup> and DESeq2.<sup>121</sup> Each requires an input of sample counts per gene or transcript that can be created with tools such as featureCounts<sup>122</sup> or htseq-count.<sup>123</sup> Raw counts generated are not suitable for comparison of expression levels. Transcript length and library read size are primary factors creating bias in such data. This high-dimensional count data are, therefore, fitted to the model and normalized by the chosen package. There are several metrics for normalization of gene expression, including RPKM (reads per kilobase per million mapped reads),<sup>124</sup> FPKM (fragments per kilobase per million mapped reads), and TPM (transcripts per kilobase million).<sup>125</sup> RPKM and related FPKM for paired-end sequences normalize gene coverage through correction of differing sample sequencing depth and RNA length. However, RPKM has been shown to be a poor metric for RNA abundance between samples.<sup>125</sup> RPKM is calculated by dividing the read counts per feature with a scaling factor (total number of reads in the sample  $\times 10^{-6}$ ) and by the length of the gene (kb). Within the sample, the RPKM values can be assessed for comparative expression analysis; however, due to the nature of the variation of library sizes between samples, RPKM values will not be comparable, leading to confusion in the literature and the use of RPKM.<sup>125</sup> TPM overcomes this by reordering the calculation, normalizing for

gene length followed by normalization for library sequencing depth. Therefore, the sum of all TPMs in each sample will be the same, unlike RPKM/FPKM. This provides the opportunity for cross-sample expression-level comparisons. With the size of the dimensional data generated for gene counts, correction of statistical validity is required; a common approach is using false discovery rate (FDR) procedures to correct for multiple tests, for example, using the Benjamini–Hochberg method.<sup>126</sup> Such processes are aimed at controlling the number of false positives when the null hypothesis has been incorrectly rejected.

#### *Differential gene analysis*

One of the most commonly used protocols with RNA-seq data analysis is the assessment of changes in expression of genes between sample conditions. Several methods have been produced to normalize and model the count data produced from aligned short reads. Generally, the input for these tools will be raw counts, to avoid biases introduced through normalization. Methods to model expression from count data include DESeq2,<sup>121</sup> Cufflinks2,<sup>119</sup> NOISeq,<sup>127</sup> and edgeR.<sup>117</sup> When working with transcript-level features, a further consideration would be the change in transcript length across samples/conditions that would alter intra-sample calculations.<sup>119</sup> Comparative analyses of techniques used for differential expression studies have been reported<sup>85,116,128,129</sup> and reviewed.<sup>84,130,131</sup> Differential expression analysis results in lists of differentially expressed genes (DEGs) or features and associated fold changes. Decision on biological significance to filter the data set relative to fold change and adjusted *p*-value thresholds is highly dependent on the experimental design, which usually will require manual interactive inspection of the data. Principal component analysis (PCA) reduces the data dimensionality down into components of variation.<sup>132</sup> By taking the main components and plotting them in either two- or three-dimensional (2D or 3D) space, samples can be visualized to enhance interpretability. PC1 describes the prominent variation within the data, PC2 the second, and so on. This aids visualization of groupings between replicates as well as potentially identifying sample outliers.

Transcript-level differential expression analysis may assist in the detection of isoform changes. Transcripts can be assembled using tools

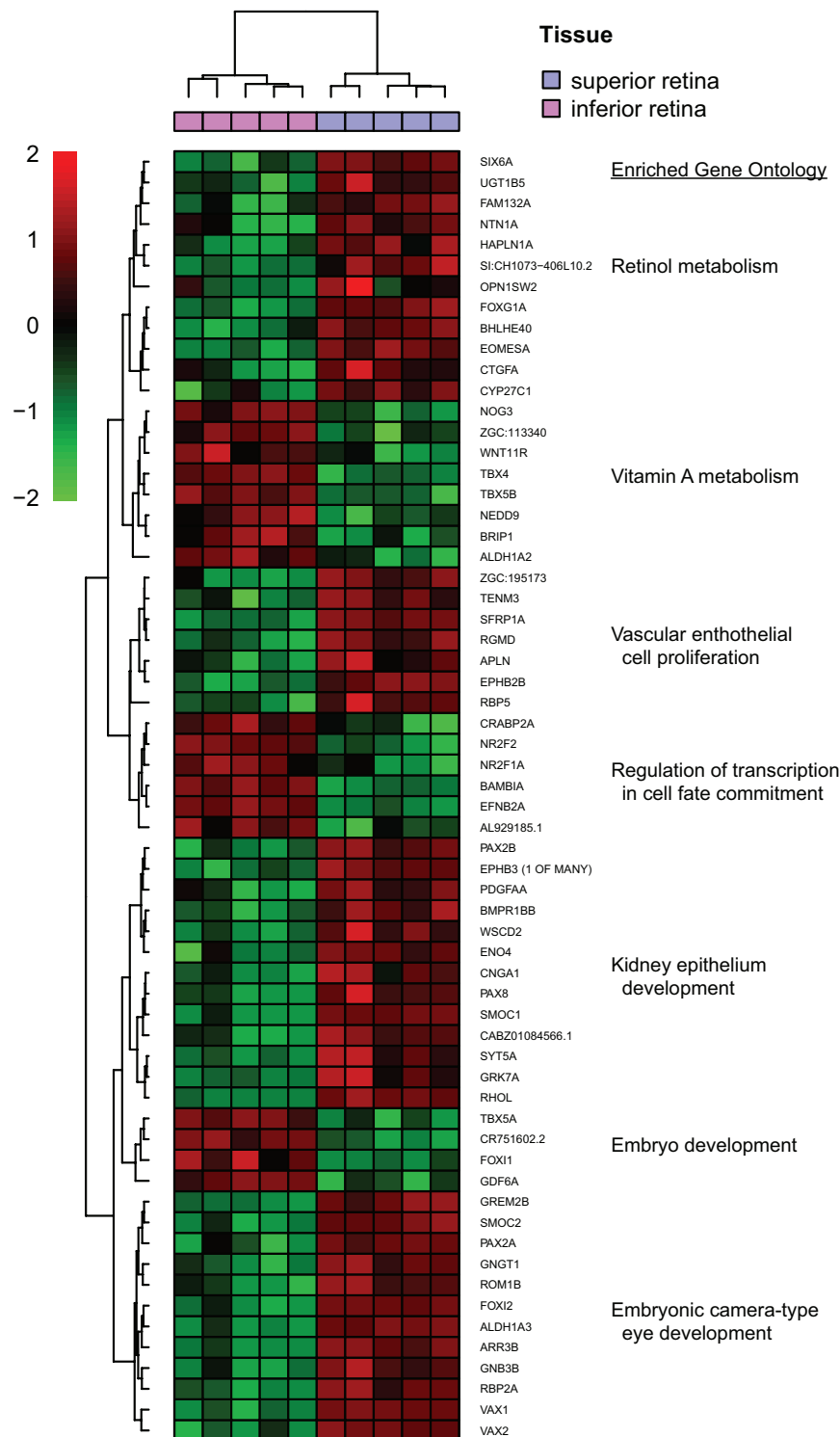


**Figure 3.** Heat map of differentially expressed genes (DEGs) in zebrafish between isolated optic fissure tissue and dorsal retina at 56 hours post fertilization (hpf),<sup>159</sup> generated by R for Statistics package NMF. DEGs were identified using DESeq2, whose output was filtered for biologically significant results using criteria of a false discovery rate of less than 0.01 and fold change greater than 2. Resulting DESeq2 analysis was rlog transformed and hierarchical clustering performed on differential gene list. The z-score scale bar represents relative expression  $\pm 2SD$  from the mean. Top enriched gene ontology for biological process (BP) is highlighted for each cluster.

including Cuffdiff2 or StringTie<sup>133</sup> that assemble reads into potential transcripts, using prior knowledge, but also will identify novel transcript isoforms, followed by comparison of expression levels. Alternative splicing occurs in 90–95% of genes in mammals; therefore, analysis of the alternative use of exons and splice sites from RNA-seq data is of vital importance.<sup>134,135</sup> Tools to assess differential usage of features such as exons or splice sites handle the information differently, using an exon-based approach, comparing to the overall expression of the associated gene.<sup>136,137</sup> Each has potential benefits and drawbacks, summarized in a recent report on the assessment of tools available.<sup>138</sup>

Batch effects can be a significant source of variation between batches of samples, resulting in reports of false DEGs. There are a number of approaches to correct for known or unknown batch effects, including surrogate variable analysis (SVA)<sup>54</sup> and ComBat.<sup>139</sup> Numerous tools have been designed with batch effect correction stages optional and evaluated.<sup>55</sup> Batch effects can ultimately range from increasing variability and reducing the power of an experiment, to becoming confounded with a desirable outcome and result in misleading biological interpretation.

#### *Data visualization*

Visualization of RNA-seq data can be achieved in several ways, similar to other forms of high-throughput sequencing data. Genome browsers such as IGV, UCSC,<sup>140</sup> and GenomeBrowse enable the user to view read alignments, highlighting read coverage and alternative splicing events with Sashimi plots, and summarizing the mapped read density over exons and junctions on the gene model.<sup>141</sup> Combined with differential expression and differential usage data, display of individual genes of biological interest at the exon level can be used to assess potential complications from read alignment artifacts, for example, specific regions of the genome remain difficult to either sequence or align to with short read sequencing.<sup>142,143</sup>

Data exploration throughout the analysis pipeline ensures precise results being reported. Useful tools for summarizing data from raw or processed sequence reads as well as alignment statistics visually include MultiQC,<sup>144</sup> QualiMap,<sup>145</sup> and RNA-SeQC.<sup>146</sup> This type of data visualization enables querying of read alignment efficiency as

well as proportions mapped to features such as exons, introns, and splice sites.

#### *Biological insight*

The biological significance of changes in the global transcriptome can be investigated through pathway enrichment of the list of DEGs/transcripts. Two example methods to aid functional significance assignment include (1) over-representation analysis (ORA), which compares the list of filtered DEGs against the annotated genome for over-represented functional assignment,<sup>147</sup> and (2) gene set enrichment analysis (GSEA), which utilizes the complete data set, ranking the entire transcriptome according to the expression-level changes using differing metrics.<sup>148</sup> Both rely heavily on prior knowledge and functional assignment to genes through Gene Ontology terms and databases such as MSigDB.<sup>148</sup> Specific tools have been created for such analysis, which invariably demonstrates gene length bias, where larger genes have a greater chance of showing significant changes. GOSeq, a Bioconductor package, aims to estimate and account for such bias.<sup>149</sup> Analytical tools continue to develop; PathwaySplice addresses explicitly bias through accounting for number of exons/junctions and performs pathway enrichment analysis.<sup>150</sup> Functional annotation data can also be readily queried using DAVID (Database for Annotation, Visualization, and Integrated Discovery),<sup>151</sup> Panther (Protein Analysis Through Evolutionary Relationships),<sup>152</sup> QuickGO,<sup>153</sup> and STRING.<sup>154</sup> ClueGO, a Cytoscape app, enables rapid querying of ontology databases, producing clustered terms in a functional network.<sup>155</sup> GSEA requires predefined collections of gene sets for analysis of the RNA-seq ranked list data set, including Kyoto Encyclopedia of Genes and Genomes (KEGG), Reactome, and BioCarta. GSEA provides a method for investigating changes in related sets of genes that may provide more insightful explanation than, for example, a large expression fold change of a single gene or numerous changes in genes with no biological theme. All genes detected experimentally are taken into consideration, not only those above the arbitrary cutoffs. Genes with small changes in expression that might not have reached the significance threshold may be of more biological importance within the same pathways, providing links between prior knowledge and newly generated experimental data.

Novel genes, as well as noncoding RNAs (ncRNA) identified in RNA-seq data sets, can present a

challenge for functional ontology assignment. Protein sequence homology can be readily assessed for protein-coding transcripts using current databases. While no standard functional annotation route is defined for ncRNAs, databases such as miRbase,<sup>156</sup> LNCipedia,<sup>157</sup> and NONCODE<sup>158</sup> maintain information on specific classes of ncRNA.

Highly similar ontologies cluster, highlighting the overall trends and themes of the underlying biological data. The expression of significant DEGs can be assessed through the generation of heat maps; a visualization method for rows of data, such as counts or expression values, related to the mean of that row. By calculating the *z*-score, the number of standard deviations from the mean expression of a gene, each sample's expression can be represented through color variations. Hierarchical clustering, a way of arranging items in a hierarchy based upon similarity, can be used alongside heat maps to produce a dendrogram that shows the relationship between the rows [in this example, genes differentially expressed during zebrafish optic fissure fusion<sup>159</sup> (Figure 3)]. One-way cluster analysis will identify clustering based upon similarity of abundant data in one dimension, such as expression patterns of genes (row) for example, whereas two-way clustering will also cluster on the second data dimension, for example, similarity of the sample profiles (column) commonly using Euclidean distances.<sup>160</sup> The aim is to identify subsets of genes in samples so that when one data dimension (gene) is used to cluster another dimension (sample), clear and significant partitions emerge.

### Reproducibility

Throughout the analysis of any data set, it is critical to maintain reproducible workflows, providing detailed information on how data are manipulated, filtered, and assessed.<sup>161,162</sup> Even so far as versions and dates of databases utilized are critical to maintain the integrity of the results. There are diverse approaches to maintaining reusable and reproducible bioinformatics pipelines such as Subversion and Git (this provides a version control system, preserving the history of the document). GitHub provides an open-source online resource for project tracking, sharing, and issue discussion. Code can also be created, shared, and annotated similarly with Jupyter scientific computing notebooks. Other options for reproducible analysis include AWS Elastic Cloud

Computing,<sup>163</sup> Docker,<sup>164</sup> and Galaxy.<sup>165</sup> Galaxy provides a web-based platform for high-throughput sequence data analysis. This platform is accessible to users without programming experience by providing a graphical web interface to command-line tools as well as predefined shared workflows and parameters. Tools and pipelines continue to develop rapidly with Galaxy adopting many of these improvements.<sup>166,167</sup>

### Utility of RNA-seq in ophthalmology research

Vision research has benefited significantly from the use of RNA-seq over recent years.<sup>168</sup> Characterization of human diseases related to the eye can prove difficult due to the lack of high-quality human tissue required for the analysis; therefore, model systems, such as animals or cell-based, provide vital resources to further our understanding of eye development and disease. The role of noncoding and circular RNAs in eye disease has been the subject of a recent review.<sup>169</sup> Here, follow some applications in ophthalmology and vision research.

#### Human retina

Transcriptome analysis of three human donor adult healthy eyes has provided insight into which RNAs are expressed specifically in human retinal tissue. Farkas and colleagues identified 79,915 novel alternative splicing events that included 29,887 novel exons and 28,271 novel exon skipping events with 116 potential novel genes expressed in retina. The observations, while highly reproducible, indicate a high level of novelty in the makeup of the retinal transcriptome that highlights the difference between species and the importance of characterization of human tissue.<sup>15</sup> Further comprehensive analysis of eight normal eyes has been carried out, demonstrating transcriptome differences between macular and peripheral retina.<sup>170</sup> Approximately, 80% of the annotated transcriptome was reported to be expressed in the retina, which showed significantly different alternative splicing patterns to the RPE, choroid, and sclera; hence, spatiotemporal gene localization is needed. Analysis of mature mRNAs and ncRNA such as long-intervening ncRNAs (lincRNAs) has been shown to be involved in numerous cellular pathways in development and disease. Analysis of total RNA within both fetal RPE and iPSC-derived RPE identified over 1000 lincRNAs and 180 novel genes

expressed in fetal RPE. The research also confirmed that the transcriptomes of iPSC-RPE were comparable to fetal RPE, so enforcing the suitability of these cells for vision research.<sup>171</sup>

While global transcriptome analysis via RNA-seq has fueled our understanding of underlying mechanisms of disease, ultimately it provides little information on the basic unit of biology, the cell. Since the development of scRNA-seq using in-house approaches, the field has seen an increase in the number of commercial options available. Protocols generally involve tissue disruption, which can lead to changes in expression profiles, although *in vivo* methods of mRNA isolation from tissue and prefiltering of cells based upon morphology and function have been produced.<sup>172–174</sup> Post hoc PCA or hierarchical clustering of single-cell data has been relied upon to determine cell type classification. Recent scRNA-seq has identified up to 40 cell types of RGCs in the mouse retina using such approaches.<sup>175</sup> While elucidation of model system RGCs has been invaluable, the need for further characterization of human cell types remains vital. To address this, human pluripotent stem-derived RGCs were profiled using scRNA-seq, showing a variable expression pattern of common RGC-associated genes, further indicating diversity within the cell population.<sup>176</sup>

### Retinal dystrophies

Currently, mutations in over 75 genes can cause retinitis pigmentosa (RP), affecting the RPE and or photoreceptor cells, leading to progressive loss of vision. Stem cell-based therapies offer potential treatment avenues, either replacement of retinal cell types through differentiation protocols or protection via general neuronal lineage cells.<sup>177</sup> Using a rat model of progressive photoreceptor degeneration harboring a mutation in the *Mertk* gene (Royal College of Surgeons, RCS rat), RNA-seq has been used to elucidate expression changes post stem-cell transplantation with human neural progenitor cells (hNPCs).<sup>178</sup> Comparative analysis of gene expression profiles of treated and untreated RCS rats and controls identified 68 genes with altered expression patterns due to treatment with hNPCs. Pathway analysis revealed an enrichment of signaling involved in phagocytic response alongside the increase in photoreceptor cell survival. The underlying *Mertk* mutation causes improper phagocytosis of photoreceptor outer segments, and restoration of phagocytosis by hNPCs is

encouraging. Similarly, mouse models of RP, including the *rd10* mouse harboring a mutation in *Pde6b*, have been used to assess transcriptional changes underlying photoreceptor degeneration.<sup>39</sup> Decreased expression of rod-specific genes was associated with a clear increase in Muller-specific gene expression, although other cell type-specific genes were dysregulated.<sup>39</sup> Interestingly, alternative splicing of 284 genes was altered in the degenerated retina, with predominantly increased exon inclusion.

### Age-related macular degeneration

Understanding the pathogenesis of age-related macular degeneration (AMD) has been challenging due to the multifactorial etiology.<sup>179</sup> AMD is characterized by RPE degeneration and consequent photoreceptor cell death. Although implicated in AMD, RPE phagocytosis has only recently been demonstrated to be dysfunctional by transcriptome analysis of RPE cells isolated from post-mortem AMD and normal age-matched control human eyes.<sup>180</sup> To explore the disease progression, rat models of AMD were assessed for temporal changes in retinal transcriptomes. Enrichment ontology analysis has provided insight into cellular differentiation and developmental processes, all differential expression events were downregulated in comparison to controls. Gene clusters identified differing gene sets at the various disease stages linked to apoptosis.<sup>181</sup> Targeted treatment of the exudative form of AMD through inhibition of vascular endothelial growth factor (VEGF) signaling using ascorbate-based targeted DNA hydroxymethylation has been validated via characterization of the resultant transcriptome in RPE cells (human fetal, rat and cell line ARPE-19) showing significant reduction in VEGF expression.<sup>182</sup>

### Corneal dystrophies

Corneal dystrophies are a group of genetic conditions that result in sight loss from various patterns of corneal opacity.<sup>183</sup> Posterior polymorphous corneal dystrophy (PPCD) is a rare autosomal dominant disorder characterized by changes in Descemet membrane and the endothelial cell layer leading to decreased vision secondary to corneal edema.<sup>183</sup> Although mutations in transcription factors *OVOL2* (type 1) and *ZEB1* (type 3) account for approximately 40% of all PPCD cases, the transcriptomes of PPCD endothelium and cultured human primary corneal endothelial

cells were assessed to further elucidate potential biomarkers.<sup>184,185</sup> Characterization of DEGs associated with *ZEB1* and *OVOL2* identified additional genes involved in proliferation, cell adhesion and migration, and cell morphology, which can be used to identify candidate genes for genetically unresolved patients.

### Glaucoma

Success in glaucoma treatment can be determined by the level of fibrotic encapsulation post trabeculectomy surgery.<sup>186</sup> To further understand the fibrotic response, RNA-seq has been used to identify dysregulated genes between primary fibrotic and nonfibrotic fibroblast cell lines isolated from glaucoma patients.<sup>187</sup> Genes involved in inflammation and apoptosis were significantly upregulated in the fibrotic cell type, including *RELB*, *PPP1R13L*, *MYOCD* (a critical cofactor of serum response factor regulating smooth muscle cell differentiation). *PRG4* was upregulated in nonfibrotic cells and has been associated with high levels of hyaluronic acid and scar-less fetal wound healing.<sup>188</sup> In total, 246 genes were differentially expressed in fibrotic cell lines compared to nonfibrotic, providing an insight to a distinct fibrosis gene signature.

### Prospects

RNA-seq is now becoming the standard method of transcriptome analysis as both the tools and technology continue to develop. Methods of analysis differ significantly and validation of results using different tools remains uncertain. As more comparative studies are evolving, more appropriate use of tools will be forthcoming. Continued development of RNA-seq technologies has resulted in the ability to analyze minimal amounts of starting material, even from older fixed and embedded archived tissue. Development of single-cell techniques continues to be a highly dynamic area of research.<sup>189–191</sup> Elucidation of cellular transcriptomes, in tissue-related context, will provide an insight into the regulation of gene expression in assumed identical cell types. Combined with temporal experimental designs, analysis of thousands of cells at a time, using techniques such as DROP-seq and InDrops, can provide detailed analysis of cellular subgroups within systems of interest.<sup>192,193</sup> Recent adaption of scRNA-seq has allowed the reconstruction of cell lineage histories in model systems.<sup>194–198</sup> Such large-scale informatics will drive knowledge

of RNA expression through developmental stages and tissue types as well as providing the technology to approach many disease-related issues.

With the availability of open-access sequence data in online repositories including NCBI SRA and EMBL ENA, combined with the increase in computing power, increasing the speed of pipeline analysis, the amount of knowledge to be gained from transcriptome analysis is increasing. Combined with other ‘omics data, RNA-seq analysis has the potential to link gene expression with genomic features such as epigenetic changes, DNA sequence alterations, and protein interactions. The Department of Health and Social Care’s 100,000 Genomes Project, whose aim was to sequence 75,000 genomes of patients with rare diseases and cancer,<sup>199,200</sup> concomitantly collected RNA alongside the DNA samples. This initiative will result in increased diagnostic rates and the discovery of novel disease-causing variants, while also providing an extensive wealth of information on transcriptomes from individuals with varied genetic backgrounds. For eye disease, the transcriptome will provide insights into how genes alter the development or function of the eye and has the potential to provide researchers with novel targets for therapeutic strategies.

### Funding

The authors disclosed receipt of the following financial support for the research, authorship, and/or publication of this article: This work was supported by The Wellcome Trust.

### Conflict of interest statement

The authors declared no potential conflicts of interest with respect to the research, authorship, and/or publication of this article.

### ORCID iD

Mariya Moosajee  <https://orcid.org/0000-0003-1688-5360>

### References

1. Wang Z, Gerstein M and Snyder M. RNA-seq: a revolutionary tool for transcriptomics. *Nat Rev Genet* 2009; 10: 57–63.
2. You J, Corley SM, Wen L, *et al.* RNA-seq analysis and comparison of corneal epithelium in keratoconus and myopia patients. *Sci Rep* 2018; 8: 389.

3. Kwon YH, Fingert JH, Kuehn MH, *et al.* Primary open-angle glaucoma. *N Engl J Med* 2009; 360: 1113–1124.
4. Weinreb RN and Khaw PT. Primary open-angle glaucoma. *Lancet* 2004; 363: 1711–1720.
5. Lozano DC, Choi D, Jayaram H, *et al.* Utilizing RNA-seq to identify differentially expressed genes in glaucoma model tissues, such as the rodent optic nerve head. *Methods Mol Biol* 2018; 1695: 299–310.
6. Teotia P, Van Hook MJ, Wichman CS, *et al.* Modeling glaucoma: retinal ganglion cells generated from induced pluripotent stem cells of patients with SIX6 risk allele show developmental abnormalities. *Stem Cells* 2017; 35: 2239–2252.
7. Yasuda M, Tanaka Y, Ryu M, *et al.* RNA sequence reveals mouse retinal transcriptome changes early after axonal injury. *PLoS ONE* 2014; 9: e93258.
8. Srivastava R, Budak G, Dash S, *et al.* Transcriptome analysis of developing lens reveals abundance of novel transcripts and extensive splicing alterations. *Sci Rep* 2017; 7: 11572.
9. Anand D, Kakrana A, Siddam AD, *et al.* RNA sequencing-based transcriptomic profiles of embryonic lens development for cataract gene discovery. *Hum Genet* 2018; 137: 941–954.
10. Sun C, Galicia C and Stenkamp DL. Transcripts within rod photoreceptors of the Zebrafish retina. *BMC Genomics* 2018; 19: 127.
11. Daum JM, Keles O, Holwerda SJ, *et al.* The formation of the light-sensing compartment of cone photoreceptors coincides with a transcriptional switch. *Elife* 2017; 6: e31437.
12. Sedykh I, Yoon B, Roberson L, *et al.* Zebrafish *zic2* controls formation of periocular neural crest and choroid fissure morphogenesis. *Dev Biol* 2017; 429: 92–104.
13. Donato L, Bramanti P, Scimone C, *et al.* miRNA expression profile of retinal pigment epithelial cells under oxidative stress conditions. *FEBS Open Bio* 2018; 8: 219–233.
14. Chen Y, Brooks MJ, Gieser L, *et al.* Transcriptome profiling of NIH3T3 cell lines expressing opsin and the P23H opsin mutant identifies candidate drugs for the treatment of retinitis pigmentosa. *Pharmacol Res* 2017; 115: 1–13.
15. Farkas MH, Grant GR, White JA, *et al.* Transcriptome analyses of the human retina identify unprecedented transcript diversity and 3.5 Mb of novel transcribed sequence via significant alternative splicing and novel genes. *BMC Genomics* 2013; 14: 486.
16. Liu Y, Zhou J and White KP. RNA-seq differential expression studies: more sequence or more replication? *Bioinformatics* 2014; 30: 301–304.
17. Tarazona S, Garcia-Alcalde F, Dopazo J, *et al.* Differential expression in RNA-seq: a matter of depth. *Genome Res* 2011; 21: 2213–2223.
18. Busby MA, Stewart C, Miller CA, *et al.* Scotty: a web tool for designing RNA-seq experiments to measure differential gene expression. *Bioinformatics* 2013; 29: 656–657.
19. Vieth B, Ziegenhain C, Parekh S, *et al.* powsimR: power analysis for bulk and single cell RNA-seq experiments. *Bioinformatics* 2017; 33: 3486–3488.
20. Wu H, Wang C and Wu Z. PROPER: comprehensive power evaluation for differential expression using RNA-seq. *Bioinformatics* 2015; 31: 233–241.
21. Hart SN, Therneau TM, Zhang Y, *et al.* Calculating sample size estimates for RNA sequencing data. *J Comput Biol* 2013; 20: 970–978.
22. Bullard JH, Purdom E, Hansen KD, *et al.* Evaluation of statistical methods for normalization and differential expression in mRNA-seq experiments. *BMC Bioinformatics* 2010; 11: 94.
23. Anders S and Huber W. Differential expression analysis for sequence count data. *Genome Biol* 2010; 11: R106.
24. Labaj PP, Leparc GG, Linggi BE, *et al.* Characterization and improvement of RNA-seq precision in quantitative transcript expression profiling. *Bioinformatics* 2011; 27: i383–i391.
25. Frazee AC, Jaffe AE, Langmead B, *et al.* Polyester: simulating RNA-seq datasets with differential transcript expression. *Bioinformatics* 2015; 31: 2778–2784.
26. Benidt S and Nettleton D. SimSeq: a nonparametric approach to simulation of RNA-sequence datasets. *Bioinformatics* 2015; 31: 2131–2140.
27. Silvester N, Alako B, Amid C, *et al.* The European nucleotide archive in 2017. *Nucleic Acids Res* 2018; 46: D36–D40.
28. Wheeler DL, Barrett T, Benson DA, *et al.* Database resources of the National Center for Biotechnology Information. *Nucleic Acids Res* 2008; 36: D13–D21.



29. Larrayoz IM, Rua O, Velilla S, *et al.* Transcriptomic profiling explains racial disparities in pterygium patients treated with doxycycline. *Invest Ophthalmol Vis Sci* 2014; 55: 7553–7561.
30. Ouyang H, Xue Y, Lin Y, *et al.* WNT7A and PAX6 define corneal epithelium homeostasis and pathogenesis. *Nature* 2014; 511: 358–361.
31. Wieben ED, Aleff RA, Tang X, *et al.* Gene expression in the corneal endothelium of Fuchs endothelial corneal dystrophy patients with and without expansion of a trinucleotide repeat in TCF4. *PLoS ONE* 2018; 13: e0200005.
32. Kabza M, Karolak JA, Rydzanicz M, *et al.* Collagen synthesis disruption and downregulation of core elements of TGF- $\beta$ , Hippo, and Wnt pathways in keratoconus corneas. *Eur J Hum Genet* 2017; 25: 582–590.
33. Sifuentes CJ, Kim JW, Swaroop A, *et al.* Rapid, dynamic activation of Muller Glial stem cell responses in zebrafish. *Invest Ophthalmol Vis Sci* 2016; 57: 5148–5160.
34. Uribe RA, Kwon T, Marcotte EM, *et al.* Id2a functions to limit Notch pathway activity and thereby influence the transition from proliferation to differentiation of retinoblasts during zebrafish retinogenesis. *Dev Biol* 2012; 371: 280–292.
35. Hoshino A, Ratnapriya R, Brooks MJ, *et al.* Molecular anatomy of the developing human retina. *Dev Cell* 2017; 43: 763.e4–779.e4.
36. Aldiri I, Xu B, Wang L, *et al.* The dynamic epigenetic landscape of the retina during development, reprogramming, and tumorigenesis. *Neuron* 2017; 94: 550.e10–568.e10.
37. Hoppe G, Yoon S, Gopalan B, *et al.* Comparative systems pharmacology of HIF stabilization in the prevention of retinopathy of prematurity. *Proc Natl Acad Sci U S A* 2016; 113: E2516–E2525.
38. Ruzycki PA, Tran NM, Kefalov VJ, *et al.* Graded gene expression changes determine phenotype severity in mouse models of CRX-associated retinopathies. *Genome Biol* 2015; 16: 171.
39. Uren PJ, Lee JT, Doroudchi MM, *et al.* A profile of transcriptomic changes in the rd10 mouse model of retinitis pigmentosa. *Mol Vis* 2014; 20: 1612–1628.
40. Whitmore SS, Wagner AH, DeLuca AP, *et al.* Transcriptomic analysis across nasal, temporal, and macular regions of human neural retina and RPE/choroid by RNA-seq. *Exp Eye Res* 2014; 129: 93–106.
41. Andrabi M, Kuraku S, Takata N, *et al.* Comparative, transcriptome analysis of self-organizing optic tissues. *Sci Data* 2015; 2: 150030.
42. Saengwimol D, Rojanaporn D, Chaitankar V, *et al.* A three-dimensional organoid model recapitulates tumorigenic aspects and drug responses of advanced human retinoblastoma. *Sci Rep* 2018; 8: 15664.
43. Kaewkhaw R, Swaroop M, Homma K, *et al.* Treatment paradigms for retinal and macular diseases using 3-D retina cultures derived from human reporter pluripotent stem cell lines. *Invest Ophthalmol Vis Sci* 2016; 57: ORSF11–ORSF11.
44. Kaewkhaw R, Kaya KD, Brooks M, *et al.* Transcriptome dynamics of developing photoreceptors in three-dimensional retina cultures recapitulates temporal sequence of human cone and rod differentiation revealing cell surface markers and gene networks. *Stem Cells* 2015; 33: 3504–3518.
45. DiStefano T, Chen HY, Panebianco C, *et al.* Accelerated and improved differentiation of retinal organoids from pluripotent stem cells in rotating-wall vessel bioreactors. *Stem Cell Reports* 2018; 10: 300–313.
46. Gill KP, Hung SS, Sharov A, *et al.* Enriched retinal ganglion cells derived from human embryonic stem cells. *Sci Rep* 2016; 6: 30552.
47. Santaguida S, Vasile E, White E, *et al.* Aneuploidy-induced cellular stresses limit autophagic degradation. *Genes Dev* 2015; 29: 2010–2021.
48. Tanenbaum ME, Stern-Ginossar N, Weissman JS, *et al.* Regulation of mRNA translation during mitosis. *Elife* 2015; 4: e07957.
49. Potapova TA, Seidel CW, Box AC, *et al.* Transcriptome analysis of tetraploid cells identifies cyclin D2 as a facilitator of adaptation to genome doubling in the presence of p53. *Mol Biol Cell* 2016; 27: 3065–3084.
50. Samuel W, Jaworski C, Postnikova OA, *et al.* Appropriately differentiated ARPE-19 cells regain phenotype and gene expression profiles similar to those of native RPE cells. *Mol Vis* 2017; 23: 60–89.
51. Radeke MJ, Radeke CM, Shih YH, *et al.* Restoration of mesenchymal retinal pigmented epithelial cells by TGF $\beta$  pathway inhibitors: implications for age-related macular degeneration. *Genome Med* 2015; 7: 58.

52. Wang J, Zibetti C, Shang P, *et al.* ATAC-seq analysis reveals a widespread decrease of chromatin accessibility in age-related macular degeneration. *Nat Commun* 2018; 9: 1364.
53. Saini JS, Corneo B, Miller JD, *et al.* Nicotinamide ameliorates disease phenotypes in a human iPSC model of age-related macular degeneration. *Cell Stem Cell* 2017; 20: 635.e7–647.e7.
54. Leek JT and Storey JD. Capturing heterogeneity in gene expression studies by surrogate variable analysis. *PLoS Genet* 2007; 3: 1724–1735.
55. Leek JT, Scharpf RB, Bravo HC, *et al.* Tackling the widespread and critical impact of batch effects in high-throughput data. *Nat Rev Genet* 2010; 11: 733–739.
56. Qiu X, Zhang H, Yu H, *et al.* Duplex-specific nuclease-mediated bioanalysis. *Trends Biotechnol* 2015; 33: 180–188.
57. Cieslik M, Chugh R, Wu YM, *et al.* The use of exome capture RNA-seq for highly degraded RNA with application to clinical cancer sequencing. *Genome Res* 2015; 25: 1372–1381.
58. O’Neil D, Glowatz H and Schlumpberger M. Ribosomal RNA depletion for efficient use of RNA-seq capacity. *Curr Protoc Mol Biol* 2013; Chapter 4, Unit 4, 19.
59. Zhao W, He X, Hoadley KA, *et al.* Comparison of RNA-seq by poly(A) capture, ribosomal RNA depletion, and DNA microarray for expression profiling. *BMC Genomics* 2014; 15: 419.
60. Picelli S, Bjorklund AK, Faridani OR, *et al.* Smart-seq2 for sensitive full-length transcriptome profiling in single cells. *Nat Methods* 2013; 10: 1096–1098.
61. Shanker S, Paulson A, Edenberg HJ, *et al.* Evaluation of commercially available RNA amplification kits for RNA sequencing using very low input amounts of total RNA. *J Biomol Tech* 2015; 26: 4–18.
62. Witwer KW and Halushka MK. Toward the promise of microRNAs – enhancing reproducibility and rigor in microRNA research. *RNA Biol* 2016; 13: 1103–1116.
63. Parekh S, Ziegenhain C, Vieth B, *et al.* The impact of amplification on differential expression analyses by RNA-seq. *Sci Rep* 2016; 6: 25533.
64. Kivioja T, Vaharautio A, Karlsson K, *et al.* Counting absolute numbers of molecules using unique molecular identifiers. *Nat Methods* 2011; 9: 72–74.
65. Islam S, Zeisel A, Joost S, *et al.* Quantitative single-cell RNA-seq with unique molecular identifiers. *Nat Methods* 2014; 11: 163–166.
66. Fu Y, Wu PH, Beane T, *et al.* Elimination of PCR duplicates in RNA-seq and small RNA-seq using unique molecular identifiers. *BMC Genomics* 2018; 19: 531.
67. Parekh S, Ziegenhain C, Vieth B, *et al.* zUMIs – a fast and flexible pipeline to process RNA sequencing data with UMIs. *GigaScience* 2018; 7: giy059.
68. Klepikova AV, Kasianov AS, Chesnokov MS, *et al.* Effect of method of deduplication on estimation of differential gene expression using RNA-seq. *PeerJ* 2017; 5: e3091.
69. Hong J and Gresham D. Incorporation of unique molecular identifiers in TruSeq adapters improves the accuracy of quantitative sequencing. *Biotechniques* 2017; 63: 221–226.
70. Adiconis X, Borges-Rivera D, Satija R, *et al.* Comparative analysis of RNA sequencing methods for degraded or low-input samples. *Nat Methods* 2013; 10: 623–629.
71. Hwang B, Lee JH and Bang D. Single-cell RNA sequencing technologies and bioinformatics pipelines. *Exp Mol Med* 2018; 50: 96.
72. Zhao S, Zhang Y, Gordon W, *et al.* Comparison of stranded and non-stranded RNA-seq transcriptome profiling and investigation of gene overlap. *BMC Genomics* 2015; 16: 675.
73. Levin JZ, Yassour M, Adiconis X, *et al.* Comprehensive comparative analysis of strand-specific RNA sequencing methods. *Nat Methods* 2010; 7: 709–715.
74. Vivancos AP, Guell M, Dohm JC, *et al.* Strand-specific deep sequencing of the transcriptome. *Genome Res* 2010; 20: 989–999.
75. Tariq MA, Kim HJ, Jejelowo O, *et al.* Whole-transcriptome RNAseq analysis from minute amount of total RNA. *Nucleic Acids Res* 2011; 39: e120.
76. Liu L, Li Y, Li S, *et al.* Comparison of next-generation sequencing systems. *J Biomed Biotechnol* 2012; 2012: 251364.
77. Metzker ML. Sequencing technologies – the next generation. *Nat Rev Genet* 2010; 11: 31–46.
78. Sims D, Sudbery I, Illott NE, *et al.* Sequencing depth and coverage: key considerations in genomic analyses. *Nat Rev Genet* 2014; 15: 121–132.
79. Zhao S, Fung-Leung WP, Bittner A, *et al.* Comparison of RNA-seq and microarray in

- transcriptome profiling of activated T cells. *PLoS ONE* 2014; 9: e78644.
80. Morrissy S, Zhao Y, Delaney A, *et al.* Digital gene expression by tag sequencing on the illumina genome analyzer. *Curr Protoc Hum Genet* 2010; Chapter11, Unit11, 1–36.
  81. Tilgner H, Grubert F, Sharon D, *et al.* Defining a personal, allele-specific, and single-molecule long-read transcriptome. *Proc Natl Acad Sci U S A* 2014; 111: 9869–9874.
  82. Baruzzo G, Hayer KE, Kim EJ, *et al.* Simulation-based comprehensive benchmarking of RNA-seq aligners. *Nat Methods* 2017; 14: 135–139.
  83. Engstrom PG, Steijger T, Sipos B, *et al.* Systematic evaluation of spliced alignment programs for RNA-seq data. *Nat Methods* 2013; 10: 1185–1191.
  84. Costa-Silva J, Domingues D and Lopes FM. RNA-seq differential expression analysis: an extended review and a software tool. *PLoS ONE* 2017; 12: e0190152.
  85. Zhang ZH, Jhaveri DJ, Marshall VM, *et al.* A comparative study of techniques for differential expression analysis on RNA-seq data. *PLoS ONE* 2014; 9: e103207.
  86. Sonesson C and Delorenzi M. A comparison of methods for differential expression analysis of RNA-seq data. *BMC Bioinformatics* 2013; 14: 91.
  87. Andrews S. FASTQC – a quality control tool for high throughput sequence data 2014, <http://www.bioinformatics.babraham.ac.uk/projects/fastqc/>
  88. Hannon. FASTX-toolkit 2010, [http://hannonlab.cshl.edu/fastx\\_toolkit/](http://hannonlab.cshl.edu/fastx_toolkit/)
  89. Bolger AM, Lohse M and Usadel B. Trimmomatic: a flexible trimmer for Illumina sequence data. *Bioinformatics* 2014; 30: 2114–2120.
  90. Krueger F. Trim Galore! 2012, [https://www.bioinformatics.babraham.ac.uk/projects/trim\\_galore/](https://www.bioinformatics.babraham.ac.uk/projects/trim_galore/)
  91. Martin M. Cutadapt removes adapter sequences from high-throughput sequencing reads. *Embnetjournal* 2011; 17: 3.
  92. Patro R, Duggal G, Love MI, *et al.* Salmon provides fast and bias-aware quantification of transcript expression. *Nat Methods* 2017; 14: 417–419.
  93. Bray NL, Pimentel H, Melsted P, *et al.* Near-optimal probabilistic RNA-seq quantification. *Nat Biotechnol* 2016; 34: 525–527.
  94. Patro R, Mount SM and Kingsford C. Sailfish enables alignment-free isoform quantification from RNA-seq reads using lightweight algorithms. *Nat Biotechnol* 2014; 32: 462–464.
  95. Yassour M, Kaplan T, Fraser HB, *et al.* Ab initio construction of a eukaryotic transcriptome by massively parallel mRNA sequencing. *Proc Natl Acad Sci U S A* 2009; 106: 3264–3269.
  96. Denoeud F, Aury JM, Da Silva C, *et al.* Annotating genomes with massive-scale RNA sequencing. *Genome Biol* 2008; 9: R175.
  97. Kim D, Langmead B and Salzberg SL. HISAT: a fast spliced aligner with low memory requirements. *Nat Methods* 2015; 12: 357–360.
  98. Huang S, Zhang J, Li R, *et al.* SOAPsplice: genome-wide ab initio detection of splice junctions from RNA-seq data. *Front Genet* 2011; 2: 46.
  99. Kim D, Pertea G, Trapnell C, *et al.* TopHat2: accurate alignment of transcriptomes in the presence of insertions, deletions and gene fusions. *Genome Biol* 2013; 14: R36.
  100. Dobin A, Davis CA, Schlesinger F, *et al.* STAR: ultrafast universal RNA-seq aligner. *Bioinformatics* 2013; 29: 15–21.
  101. Group TSBFSW. Sequence alignment/map format specification 2009, <https://samtools.github.io/hts-specs/SAMv1.pdf>
  102. Thorvaldsdottir H, Robinson JT and Mesirov JP. Integrative Genomics Viewer (IGV): high-performance genomics data visualization and exploration. *Brief Bioinform* 2013; 14: 178–192.
  103. Robinson JT, Thorvaldsdottir H, Winckler W, *et al.* Integrative genomics viewer. *Nat Biotechnol* 2011; 29: 24–26.
  104. Bozeman MGH. Golden Helix GenomeBrowse® visualization tool (Version 3), 2018, <http://goldenhelix.com/products/GenomeBrowse/index.html>
  105. Wu DC, Yao J, Ho KS, *et al.* Limitations of alignment-free tools in total RNA-seq quantification. *BMC Genomics* 2018; 19: 510.
  106. Kozarewa I, Ning Z, Quail MA, *et al.* Amplification-free Illumina sequencing-library preparation facilitates improved mapping and assembly of (G+C)-biased genomes. *Nat Methods* 2009; 6: 291–295.
  107. Lahens NF, Kavakli IH, Zhang R, *et al.* IVT-seq reveals extreme bias in RNA sequencing. *Genome Biol* 2014; 15: R86.

108. Broad Institute. Picard toolkit, 2018, <https://broadinstitute.github.io/picard/>
109. Dozmorov MG, Adrianto I, Giles CB, *et al.* Detrimental effects of duplicate reads and low complexity regions on RNA- and ChIP-seq data. *BMC Bioinformatics* 2015; 16(Suppl. 13): S10.
110. Aird D, Ross MG, Chen WS, *et al.* Analyzing and minimizing PCR amplification bias in Illumina sequencing libraries. *Genome Biol* 2011; 12: R18.
111. Benjamini Y and Speed TP. Summarizing and correcting the GC content bias in high-throughput sequencing. *Nucleic Acids Res* 2012; 40: e72.
112. Hansen KD, Brenner SE and Dudoit S. Biases in Illumina transcriptome sequencing caused by random hexamer priming. *Nucleic Acids Res* 2010; 38: e131.
113. Li H, Handsaker B, Wysoker A, *et al.* The Sequence alignment/map format and SAMtools. *Bioinformatics* 2009; 25: 2078–2079.
114. Sena JA, Galotto G, Devitt NP, *et al.* Unique Molecular Identifiers reveal a novel sequencing artefact with implications for RNA-seq based gene expression analysis. *Sci Rep* 2018; 8: 13121.
115. Marioni JC, Mason CE, Mane SM, *et al.* RNA-seq: an assessment of technical reproducibility and comparison with gene expression arrays. *Genome Res* 2008; 18: 1509–1517.
116. Kvam VM, Liu P and Si Y. A comparison of statistical methods for detecting differentially expressed genes from RNA-seq data. *Am J Bot* 2012; 99: 248–256.
117. Robinson MD, McCarthy DJ and Smyth GK. edgeR: a Bioconductor package for differential expression analysis of digital gene expression data. *Bioinformatics* 2010; 26: 139–140.
118. Hardcastle TJ and Kelly KA. baySeq: empirical Bayesian methods for identifying differential expression in sequence count data. *BMC Bioinformatics* 2010; 11: 422.
119. Trapnell C, Hendrickson DG, Sauvageau M, *et al.* Differential analysis of gene regulation at transcript resolution with RNA-seq. *Nat Biotechnol* 2013; 31: 46–53.
120. Trapnell C, Roberts A, Goff L, *et al.* Differential gene and transcript expression analysis of RNA-seq experiments with TopHat and Cufflinks. *Nat Protoc* 2012; 7: 562–578.
121. Love MI, Huber W and Anders S. Moderated estimation of fold change and dispersion for RNA-seq data with DESeq2. *Genome Biol* 2014; 15: 550.
122. Liao Y, Smyth GK and Shi W. featureCounts: an efficient general purpose program for assigning sequence reads to genomic features. *Bioinformatics* 2014; 30: 923–930.
123. Anders S, Pyl PT and Huber W. HTSeq—a Python framework to work with high-throughput sequencing data. *Bioinformatics* 2015; 31: 166–169.
124. Mortazavi A, Williams BA, McCue K, *et al.* Mapping and quantifying mammalian transcriptomes by RNA-seq. *Nat Methods* 2008; 5: 621–628.
125. Wagner GP, Kin K and Lynch VJ. Measurement of mRNA abundance using RNA-seq data: RPKM measure is inconsistent among samples. *Theory Biosci* 2012; 131: 281–285.
126. Benjamini YYH. Controlling the false discovery rate – a practical and powerful approach to multiple testing. *J Roy Stat Soc B Met* 1995; 51: 289–300.
127. Tarazona S, Furio-Tari P, Turra D, *et al.* Data quality aware analysis of differential expression in RNA-seq with NOISeq R/Bioc package. *Nucleic Acids Res* 2015; 43: e140.
128. Garber M, Grabherr MG, Guttman M, *et al.* Computational methods for transcriptome annotation and quantification using RNA-seq. *Nat Methods* 2011; 8: 469–477.
129. Dillies MA, Rau A, Aubert J, *et al.* A comprehensive evaluation of normalization methods for Illumina high-throughput RNA sequencing data analysis. *Brief Bioinform* 2013; 14: 671–683.
130. Seyednasrollah F, Laiho A and Elo LL. Comparison of software packages for detecting differential expression in RNA-seq studies. *Brief Bioinform* 2015; 16: 59–70.
131. Conesa A, Madrigal P, Tarazona S, *et al.* A survey of best practices for RNA-seq data analysis. *Genome Biol* 2016; 17: 13.
132. Zeng ISL and Lumley T. Review of statistical learning methods in integrated omics studies (an integrated information science). *Bioinform Biol Insights* 2018; 12: 1–16.
133. Pertea M, Kim D, Pertea GM, *et al.* Transcript-level expression analysis of RNA-seq experiments with HISAT, StringTie and Ballgown. *Nat Protoc* 2016; 11: 1650–1667.
134. Wang ET, Sandberg R, Luo S, *et al.* Alternative isoform regulation in human

- tissue transcriptomes. *Nature* 2008; 456: 470–476.
135. Pan Q, Shai O, Lee LJ, *et al.* Deep surveying of alternative splicing complexity in the human transcriptome by high-throughput sequencing. *Nat Genet* 2008; 40: 1413–1415.
  136. Hartley SW and Mullikin JC. Detection and visualization of differential splicing in RNA-seq data with JunctionSeq. *Nucleic Acids Res* 2016; 44: e127.
  137. Anders S, Reyes A and Huber W. Detecting differential usage of exons from RNA-seq data. *Genome Res* 2012; 22: 2008–2017.
  138. Hooper JE. A survey of software for genome-wide discovery of differential splicing in RNA-seq data. *Hum Genomics* 2014; 8: 3.
  139. Johnson WE, Li C and Rabinovic A. Adjusting batch effects in microarray expression data using empirical Bayes methods. *Biostatistics* 2007; 8: 118–127.
  140. Casper J, Zweig AS, Villarreal C, *et al.* The UCSC genome browser database: 2018 update. *Nucleic Acids Res* 2018; 46: D762–D769.
  141. Katz Y, Wang ET, Silterra J, *et al.* Quantitative visualization of alternative exon expression from RNA-seq data. *Bioinformatics* 2015; 31: 2400–2402.
  142. Treangen TJ and Salzberg SL. Repetitive DNA and next-generation sequencing: computational challenges and solutions. *Nat Rev Genet* 2011; 13: 36–46.
  143. Goldfeder RL, Priest JR, Zook JM, *et al.* Medical implications of technical accuracy in genome sequencing. *Genome Med* 2016; 8: 24.
  144. Ewels P, Magnusson M, Lundin S, *et al.* MultiQC: summarize analysis results for multiple tools and samples in a single report. *Bioinformatics* 2016; 32: 3047–3048.
  145. Okonechnikov K, Conesa A and Garcia-Alcalde F. Qualimap 2: advanced multi-sample quality control for high-throughput sequencing data. *Bioinformatics* 2016; 32: 292–294.
  146. DeLuca DS, Levin JZ, Sivachenko A, *et al.* RNA-SeQC: RNA-seq metrics for quality control and process optimization. *Bioinformatics* 2012; 28: 1530–1532.
  147. Tavazoie S, Hughes JD, Campbell MJ, *et al.* Systematic determination of genetic network architecture. *Nat Genet* 1999; 22: 281–285.
  148. Subramanian A, Tamayo P, Mootha VK, *et al.* Gene set enrichment analysis: a knowledge-based approach for interpreting genome-wide expression profiles. *Proc Natl Acad Sci U S A* 2005; 102: 15545–15550.
  149. Young MD, Wakefield MJ, Smyth GK, *et al.* Gene ontology analysis for RNA-seq: accounting for selection bias. *Genome Biol* 2010; 11: R14.
  150. Yan A, Ban Y, Gao Z, *et al.* PathwaySplice: an R package for unbiased pathway analysis of alternative splicing in RNA-seq data. *Bioinformatics* 2018; 34: 3220–3222.
  151. Huang da W, Sherman BT and Lempicki RA. Systematic and integrative analysis of large gene lists using DAVID bioinformatics resources. *Nat Protoc* 2009; 4: 44–57.
  152. Bellone RR, Holl H, Setaluri V, *et al.* Evidence for a retroviral insertion in TRPM1 as the cause of congenital stationary night blindness and leopard complex spotting in the horse. *PLoS ONE* 2013; 8: e78280.
  153. Binns D, Dimmer E, Huntley R, *et al.* QuickGO: a web-based tool for Gene Ontology searching. *Bioinformatics* 2009; 25: 3045–3046.
  154. Szklarczyk D, Franceschini A, Wyder S, *et al.* STRING v10: protein-protein interaction networks, integrated over the tree of life. *Nucleic Acids Res* 2015; 43: D447–D452.
  155. Bindea G, Mlecnik B, Hackl H, *et al.* ClueGO: a Cytoscape plug-in to decipher functionally grouped gene ontology and pathway annotation networks. *Bioinformatics* 2009; 25: 1091–1093.
  156. Kozomara A and Griffiths-Jones S. miRBase: annotating high confidence microRNAs using deep sequencing data. *Nucleic Acids Res* 2014; 42: D68–D73.
  157. Volders PJ, Helsens K, Wang X, *et al.* LNCipedia: a database for annotated human lncRNA transcript sequences and structures. *Nucleic Acids Res* 2013; 41: D246–D251.
  158. Fang S, Zhang L, Guo J, *et al.* NONCODEV5: a comprehensive annotation database for long non-coding RNAs. *Nucleic Acids Res* 2018; 46: D308–D314.
  159. Richardson R, Owen N, Toms M, *et al.* Transcriptome profiling of zebrafish optic fissure fusion. *Sci Rep* 2019; 9: 1541.
  160. D’Haeseleer P. How does gene expression clustering work? *Nature Biotechnology* 2005; 23: 1499.
  161. Consortium SM-I. A comprehensive assessment of RNA-seq accuracy, reproducibility and information content by the Sequencing Quality

- Control Consortium. *Nat Biotechnol* 2014; 32: 903–914.
162. Nekrutenko A and Taylor J. Next-generation sequencing data interpretation: enhancing reproducibility and accessibility. *Nat Rev Genet* 2012; 13: 667–672.
163. Amazon. Amazon Web Services Elastic Compute resource, 2018, <http://aws.amazon.com/ec2/>
164. Jensen TL, Frasketi M, Conway K, *et al.* RSEQREP: RNA-seq Reports, an open-source cloud-enabled framework for reproducible RNA-seq data processing, analysis, and result reporting. *F1000Res* 2017; 6: 2162.
165. Afgan E, Baker D, Batut B, *et al.* The Galaxy platform for accessible, reproducible and collaborative biomedical analyses: 2018 update. *Nucleic Acids Res* 2018; 46: W537–W544.
166. Fisch KM, Meissner T, Gioia L, *et al.* Omics pipe: a community-based framework for reproducible multi-omics data analysis. *Bioinformatics* 2015; 31: 1724–1728.
167. Gruning BA, Fallmann J, Yusuf D, *et al.* The RNA workbench: best practices for RNA and high-throughput sequencing bioinformatics in Galaxy. *Nucleic Acids Res* 2017; 45: W560–W566.
168. Yang HJ, Ratnapriya R, Cogliati T, *et al.* Vision from next generation sequencing: multi-dimensional genome-wide analysis for producing gene regulatory networks underlying retinal development, aging and disease. *Prog Retin Eye Res* 2015; 46: 1–30.
169. Wawrzyniak O, Zarebska Z, Rolle K, *et al.* Circular and long non-coding RNAs and their role in ophthalmologic diseases. *Acta Biochim Pol* 2018; 65: 497–508.
170. Li M, Jia C, Kazmierkiewicz KL, *et al.* Comprehensive analysis of gene expression in human retina and supporting tissues. *Hum Mol Genet* 2014; 23: 4001–4014.
171. Au ED, Fernandez-Godino R, Kaczynski TJ, *et al.* Characterization of lincRNA expression in the human retinal pigment epithelium and differentiated induced pluripotent stem cells. *PLoS ONE* 2017; 12: e0183939.
172. Gross A, Schoendube J, Zimmermann S, *et al.* Technologies for single-cell isolation. *Int J Mol Sci* 2015; 16: 16897–16919.
173. Lovatt D, Ruble BK, Lee J, *et al.* Transcriptome in vivo analysis (TIVA) of spatially defined single cells in live tissue. *Nat Methods* 2014; 11: 190–196.
174. Laboissonniere LA, Sonoda T, Lee SK, *et al.* Single-cell RNA-seq of defined subsets of retinal ganglion cells. *J Vis Exp* 2017; 123: e55229.
175. Rheaume BA, Jereen A, Bolisetty M, *et al.* Single cell transcriptome profiling of retinal ganglion cells identifies cellular subtypes. *Nat Commun* 2018; 9: 2759.
176. Langer KB, Ohlemacher SK, Phillips MJ, *et al.* Retinal ganglion cell diversity and subtype specification from human pluripotent stem cells. *Stem Cell Reports* 2018; 10: 1282–1293.
177. Lu B, Lin Y, Tsai Y, *et al.* A subsequent human neural progenitor transplant into the degenerate retina does not compromise initial graft survival or therapeutic efficacy. *Transl Vis Sci Technol* 2015; 4: 7.
178. Jones MK, Lu B, Saghizadeh M, *et al.* Gene expression changes in the retina following subretinal injection of human neural progenitor cells into a rodent model for retinal degeneration. *Mol Vis* 2016; 22: 472–490.
179. Ambati J and Fowler BJ. Mechanisms of age-related macular degeneration. *Neuron* 2012; 75: 26–39.
180. Inana G, Murat C, An W, *et al.* RPE phagocytic function declines in age-related macular degeneration and is rescued by human umbilical tissue derived cells. *J Transl Med* 2018; 16: 63.
181. Telegina DV, Korbolina EE, Ershov NI, *et al.* Identification of functional networks associated with cell death in the retina of OXYS rats during the development of retinopathy. *Cell Cycle* 2015; 14: 3544–3556.
182. Sant DW, Camarena V, Mustafi S, *et al.* Ascorbate suppresses VEGF expression in retinal pigment epithelial cells. *Invest Ophthalmol Vis Sci* 2018; 59: 3608–3618.
183. Weiss JS, Moller HU, Aldave AJ, *et al.* IC3D classification of corneal dystrophies – edition 2. *Cornea* 2015; 34: 117–159.
184. Chung DD, Frausto RF, Lin BR, *et al.* Transcriptomic profiling of posterior polymorphous corneal dystrophy. *Invest Ophthalmol Vis Sci* 2017; 58: 3202–3214.
185. Frausto RF, Le DJ and Aldave AJ. Transcriptomic analysis of cultured corneal endothelial cells as a validation for their use in cell replacement therapy. *Cell Transplant* 2016; 25: 1159–1176.
186. Addicks EM, Quigley HA, Green WR, *et al.* Histologic characteristics of filtering blebs in glaucomatous eyes. *Arch Ophthalmol* 1983; 101: 795–798.

187. Yu-Wai-Man C, Owen N, Lees J, *et al.* Genome-wide RNA-sequencing analysis identifies a distinct fibrosis gene signature in the conjunctiva after glaucoma surgery. *Sci Rep* 2017; 7: 5644.
188. Lorenz HP and Adzick NS. Scarless skin wound repair in the fetus. *West J Med* 1993; 159: 350–355.
189. Zhu S, Qing T, Zheng Y, *et al.* Advances in single-cell RNA sequencing and its applications in cancer research. *Oncotarget* 2017; 8: 53763–53779.
190. Ooi CC, Mantalas GL, Koh W, *et al.* High-throughput full-length single-cell mRNA-seq of rare cells. *PLoS ONE* 2017; 12: e0188510.
191. Huang X, Liu S, Wu L, *et al.* High throughput single cell RNA sequencing, bioinformatics analysis and applications. *Adv Exp Med Biol* 2018; 1068: 33–43.
192. Macosko EZ, Basu A, Satija R, *et al.* Highly parallel genome-wide expression profiling of individual cells using nanoliter droplets. *Cell* 2015; 161: 1202–1214.
193. Klein AM, Mazutis L, Akartuna I, *et al.* Droplet barcoding for single-cell transcriptomics applied to embryonic stem cells. *Cell* 2015; 161: 1187–1201.
194. Fincher CT, Wurtzel O, de Hoog T, *et al.* Cell type transcriptome atlas for the planarian *Schmidtea mediterranea*. *Science* 2018; 360: eaaq1736.
195. Plass M, Solana J, Wolf FA, *et al.* Cell type atlas and lineage tree of a whole complex animal by single-cell transcriptomics. *Science* 2018; 360: eaaq1723.
196. Farrell JA, Wang Y, Riesenfeld SJ, *et al.* Single-cell reconstruction of developmental trajectories during zebrafish embryogenesis. *Science* 2018; 360: eaar3131.
197. Briggs JA, Weinreb C, Wagner DE, *et al.* The dynamics of gene expression in vertebrate embryogenesis at single-cell resolution. *Science* 2018; 360: eaar5780.
198. Wagner DE, Weinreb C, Collins ZM, *et al.* Single-cell mapping of gene expression landscapes and lineage in the zebrafish embryo. *Science* 2018; 360: 981–987.
199. England G. The 100,000 genomes project by numbers, 2018, <https://www.genomicsengland.co.uk/the-100000-genomes-project-by-numbers/>
200. Peplow M. The 100,000 genomes project. *BMJ* 2016; 353: i1757.

Visit SAGE journals online  
[journals.sagepub.com/  
 home/oed](https://journals.sagepub.com/home/oed)

 SAGE journals